



Artificial neural network model for prediction of viscoelastic behaviour of polycarbonate composites

Shriram S. Sonawane* • Sarita J. Charde • Manjakuppam Malika • Parag Thakur

Department of Chemical Engineering, 206, Nano Research Project Laboratory,
Visvesvaraya National Institute of Technology, Nagpur, MS 440010, India

Received 06 30 2020; accepted 11 17 2021

Available 04 30 2022

Abstract: Polymer composites are created by incorporating nanoparticles into polymers and can result in significant gains even with a very tiny amount of reinforcement that can be tailored to specific purposes. To have a better understanding of the behavior of these polymer composites, a variety of characterizations and analysis must be conducted, which demands financial and time investment. Thus, computational techniques can be beneficial in reducing the number of characterizations and studies required to produce polymer composites. Prediction of thermomechanical characteristics has been made possible using a computational technology known as an artificial neural network (ANN). The present study used dynamic mechanical analysis (DMA) to characterise polycarbonate / calcium carbonate-SiO₂ core shell composites (polycarbonate composites). The chosen ANN model comprised a network of [2-4-1] (Inputs to the input layer – Neural network count in the hidden layer – Output from the output layer) based on the dataset. Prediction accuracy was approximately 90% when utilising the ANN approach. The applicability and performance of ANN were also confirmed using mean squared error (MSE), which is in the range of 10⁻⁵ in this scenario. Correlation coefficient of 0.999 was found between the output predicted by ANN and the actual output. Additionally, sensitivity analysis established the importance of various input variables in terms of output. Optimizing the variables enabled maximization of the circumstances, hence anticipating the glass transition temperature.

Keywords: Artificial neural network (ANN), polycarbonate composites, dynamic mechanical analyzer, glass transition temperature, storage modulus

*Corresponding author.

E-mail address: shriramsonawane@gmail.com (Shriram S. Sonawane).

Peer Review under the responsibility of Universidad Nacional Autónoma de México.

1. Introduction

Polycarbonate composites are used in a variety of industries, including building, vehicles, aerospace, consumer electronics, and packaging. To determine the applications, it is necessary to analyze the thermal stability, mechanical strength, wear resistance, viscoelastic behavior, and flame resistance of nanoparticles, as well as their topography, size, and dispersion (Charde Sonawane, Sonawane & Shimpi, 2018; Khan et al., 2019). It is based on a series of experiments conducted with sophisticated tools that are both expensive and time intensive. When considering mechanical strength at changing temperatures, thermo-mechanical qualities are one of the critical factors that determine the application of polymer composites (Ghanshyam, Sonawane et al., 2016).

Thermomechanical properties are investigated with the use of a dynamic mechanical analyzer (DMA). These dynamic tests are beneficial in the investigation of polymeric materials' viscoelasticity. It expresses material stiffness and damping as storage modulus and tan delta. It is a measure of the degree of crosslinking between nanoparticles and the polymer matrix, expressed as a glass transition temperature. (Landge et al., 2021). The enhancement of thermomechanical characteristics is dependent on the interaction between matrix and filler, the extent of cross linking, and crystallinity. The storage modulus and damping behavior of the composites have been reported to rise or decrease with the addition of nano-fillers (Ghanshyam et al., 2016a; Ghanshyam et al., 2017).

Polycarbonate composites exhibit a wide range of thermomechanical properties that vary according to the type of nanofiller, organic modifier, composite synthesis method, and processing conditions. According to the literature, polycarbonate clay composites displayed superior qualities when modified with phosphonium salts rather than ammonium salts (Suin, et al. 2013). The dynamic mechanical characteristics of polycarbonate with ammonium modified clay nanofillers synthesized via melt extrusion did not improve (Carrion et al. 2008). Polycarbonate reinforced with nanoparticles of silica produced via melt intercalation was projected to have improved thermo-mechanical characteristics. Due to the existence of hydrogen bonding, the strong interaction between the carbonyl group in the PC and the hydroxide group on silica results in the increase of characteristics. Thus, the effect of silica nanoparticle modification does not result in a significant change in dynamic mechanical characteristics (Luyt et al., 2011). Additionally, a decrease in thermomechanical characteristics was seen for PC/carbon nanotubes (Jin et al., 2008) as well as PC/ ZnO (Carrion et al. 2007; Charde et al., 2017). In another case, thermomechanical characteristics of PC/silica composites

made by blending and melt pressing were found to be improved when compared to pure PC for 1% and 2% composites (Chau et al., 2010; Motaung et al., 2012).

The idea of lowering testing effort has been examined consistently by scientists, and after a great deal of work, computational procedures have been established as the optimum option. It was able to limit the number of analyses in order to obtain a rough notion of how composites behave. In the instance of an artificial neural network (ANN), a computational technique, a subset of experimental data is used to accurately anticipate the behaviour of a substance without conducting detailed testing (Mishra et al. 2009a; Mishra et al. 2009b).

In material research, ANNs have been effectively utilised to forecast characteristics of materials. The dynamic mechanical characteristics of PTFE-based short carbon fibre composites were determined using ANN. It was determined that a sizable dataset was required due to the complexity of the relationship between the input and output (Zhang et al., 2002a). A study utilising ANN and SVR on polymer clay composites demonstrated a link between the thermo-mechanical characteristics and composition of the clay and temperature. The anticipated model was said to be advantageous for producing polymer clay composites with desired mechanical properties (Majid & Lee, 2009). Another study used an ANN technique called Radial basis functional network to investigate polymer-clay/silica hybrid composites. It was established that such methods could be used to forecast the properties of composites (lingaraju et al., 2011). The thermomechanical characteristics of a system of PC-clay nanocomposites were predicted using ANN using only the input variable as storage modulus (Charde & Sonawane, 2016).

The present study examines the thermomechanical characteristics of polycarbonate/caco3-silica core shell composites (polycarbonate composites), utilising input and output data from DMA results for polycarbonate composites generated via melt extrusion. The purpose of this study was to determine the ability of artificial neural networks to anticipate and simplify in order to estimate thermomechanical characteristics. A model (ANN) was constructed to facilitate the study of the thermomechanical properties of polycarbonate composites, hence reducing the number of experiments required and aiding in the understanding of such composites' behavior (Malika & Sonawane, 2021a; Malika & Sonawane, 2021b; Shimpi, Khan et al., 2018).

Such ANN models facilitated the identification of composites' potential without the need for tests. This could result in cost and time savings associated with material characterization and analysis (Aktay et al., 2005; Majid & Lee, 2009; Khan & Khan, 2002).

2. Materials and methods

2.1. Materials

CaCO₃ nanoparticles were synthesized and used after drying. Na₂SiO₃·9H₂O, and HCl used in the experiments were of analytical purity and were used as obtained. Polycarbonate (MAKROLON® 2407) was purchased from Bayer, India.

2.2. Synthesis and modification of nanoparticle

The Na₂SiO₃ solution was added to the slurry of CaCO₃ nanoparticles in a mole ratio of SiO₂/CaCO₃ of 1:5. Heating the mixture to 80°C and monitoring the pH continuously until a pH of 7 was achieved. The slurry was aged for two hours. CaCO₃ SiO₂ core shell nanoparticles were obtained by washing the slurry, filtration, and drying.

Stearic acid was used to modify the product. Drying nanoscale CaCO₃/SiO₂ core shell nanoparticles at 100°C for 12 hours to remove any absorbed moisture. Stearic acid (0.002 mol) was dissolved in 100 ml pure toluene and then transferred to a flask equipped with a stirrer. Around 5g of CaCO₃/SiO₂ core shell nanoparticles were slowly added over a 10-minute period with vigorous stirring (2,500 rpm). After the particles were completely added to the mixing chamber, the materials were mixed for an additional hour with continuous stirring. After grinding the product, a fine powder of stearic acid-coated CaCO₃/SiO₂ core shell nanoparticles was obtained. (Sonawane et al., 2011; Zhang & Li, 2004).

2.3. Polycarbonate composites

Melt extrusion at 280°C and 100 rpm was used to fabricate polycarbonate composites. The injector was maintained at 310°C and filled with melt polymer. The mould was kept at 145°C, the moulding pressure was approximately 900 bars for 7 seconds, and the post pressure was approximately 650 bars for 5 seconds. Prior to mixing, the PC pellets were dried at 80°C for 12 hours, and the PC was gradually fed with 5g of PC and the corresponding percentage of nanoparticles. The use of counter current screws and recycling for three minutes should ensure adequate mixing of nanoparticles into the polycarbonate matrix. Composites were moulded to a 50x10x1 mm³ dimension for the purpose of evaluating their thermomechanical properties.

2.4. Characterization methods

2.4.1. XRD

After thoroughly cleaning the sample holder, the nano powder was spread on the sample holder. The sample was then placed inside the XRD machine (Model-DY-1656) and the sample was investigated to understand the phase(s) and size of the nano powder.

2.4.2. SEM

The sample of nano powder was affixed to a metallic stub which is placed on the sample holder. There is a fixed sample holder inside the machine on a rotatable disc. The nano powders were thus made ready for SEM. The equipment used was SEM (JEOL-JSM 5800), to study the morphology of the nanoparticles operated under low vacuum at an accelerating voltage of 25 kV to get the sharp image of the sample.

2.4.3. TGA

From TGA, the data on weight loss and decomposition of the samples with temperature is available. Thermo-gravimetric analyzer was TG 6300 type analyzer (SII Nanotechnology Incorporation, Japan) under the inert atmosphere with nitrogen at the rate of 60-100 ml/min. About 2 to 10 mg of the sample were heated from 25 to 800°C at a heating rate of 10°C.

2.4.4. DSC

DSC 7020, AS-3D, SII Nanotechnology Inc., Japan was used to determine the glass transition temperature (T_g). The analysis was carried out under inert atmosphere at a rate of 60 – 100 ml/min using 5-10 mg of sample. It involves heating the samples from 25°C to 550°C at a rate of 10°C/ min. 5 mg of the sample was taken in an aluminium pan and sealed for the DSC analysis.

2.4.5. DMA

DMA Q 800, TA Instruments Inc., USA, was used to study the storage modulus and tan δ. Temperature range was 40-170°C and the rate of heating was 3°C/ min in an ambient condition. The specimens were prepared by injection molding machine “HAAKE Mini CTW” and had the dimension 50x10x1mm³. Analysis was carried out at a constant vibration frequency of 1 Hz, using a single cantilever clamp.

2.5. Computational method

The biological nervous system stimulates an artificial neural network that is being used as a tool. Similar to the brain, it is capable of recognizing patterns within data. Numerous processing units (or artificial neurons) are connected in a predetermined manner to perform a desired pattern recognition task (Yegnanarayana, 2003). Neurons are organized into three layers: input, hidden, and output. The input layer is the one that receives the input dataset. The hidden layer functions as the system's brain. The target layer determines the system's final output, referred to as the output layer. The neurons and their interconnections adjust the input data at each step to produce the output. Additionally, one or more layers of hidden neurons can be used (Nasir et al., 2009). Each neuron has the ability to transmit data to the next neuron. The output of a preceding neuron is multiplied by the

weight, then modified using function, and finally deviated by the bias. Throughout the training period, system changes result in weight and bias adjustments to achieve optimal performance. Finally, the model's performance is quantified using the mean squared error (MSE) (Zhang et al., 2002b). The equation used to attain the output for a neuron t is given as below,

$$t = a(\sum_{i=1}^n w_i x_i - b) \tag{1}$$

Where x_i signifies the i^{th} weight, b denotes the bias and, a signifies the transfer function. Here a feed forward neural network with three layers was chosen. The transfer function being tangent sigmoid (tansig) for the hidden layer. A linear transfer function (purelin) was selected for the output layer. The log sigmoid function is determined by eq. 2 and tansigmoid by eq. 3.

$$f(x) = \frac{1}{1 + e^{-x}} \tag{2}$$

$$\text{tansig}(x) = \frac{2}{1 + e^{-2x}} - 1 \tag{3}$$

where linear activation function is given by eq. 4

$$f(x) = x \tag{4}$$

The performance of ANN model was evaluated in terms of mean squared error (MSE) as given by eq. 5

$$MSE = \sqrt{\frac{\sum_{i=1}^n (y_{i,e} - y_{i,p})^2}{n}} \tag{5}$$

Where, n is the number of experimental data, the experimental data is denoted as $Y_{i,e}$ and the corresponding predicted data denoted as $Y_{i,p}$.

We have used MATLAB based ANN toolbox, version R2012a ("Matlab neural network toolbox, <http://www.mathworks.com/products/neural-network>," n.d.) for developing the model. This tool provides supervised learning. This tool is a combination of feedforward, backpropagation, radial basis, and dynamic networks (Khanam et al., 2016). A sensitivity analysis is useful for the evaluation of the comparative significance of each input variable on the output and is given by Garson (1991),

$$I_j = \frac{\sum_{m=1}^{m=N_h} h \left(\left(\frac{|w_{jm}^{ih}|}{\sum_{k=1}^{N_i} |w_{km}^{ih}|} \right) \times |w_{mn}^{ho}| \right)}{\sum_{k=1}^{k=N_i} \left\{ \sum_{m=1}^{m=N_h} h \left(\frac{|w_{km}^{ih}|}{\sum_{k=1}^{N_i} |w_{km}^{ih}|} \right) \times |w_{mn}^{ho}| \right\}} \tag{6}$$

where, the comparative implication of the j^{th} input variable on the output variable is I_j . The number of input neurons is N_i and hidden neurons is N_h . The connection weight is W . The input, hidden and output layers are denoted by the superscripts l , h and o respectively. The input, hidden and output neurons are represented by the subscripts k , m and n respectively.

2.6. Proposed Methodology

We are considering that percentage composition of nanoparticles and temperature influences the output that is $\tan \delta$ and finally glass transition. The system is a polycarbonate/ calcium carbonate-silica core shell composites with varying concentration of nanoparticles such as 1%, 3% and 5%. The damping effect ($\tan \delta$) is considered as a nonlinear function of percentage of nanoparticles and temperature. Additionally, for fast learning of the model, we consider transition temperature at zero percentage nanoparticles composition (pure PC). It is only one and constant value obtained from loss tangent ($\tan \delta$) peak point (Khan et al., 2009). We are using MATLAB, R2012a which applies supervised and feed forward back propagation via neural network tool.

3. Results and discussion

3.1. SEM

The nanoparticles were analysed using SEM images and found to be hexagonal, cube-like crystals. Figure.1 is the image of $\text{CaCO}_3/\text{SiO}_2$ core shell nanoparticles which are hexagonal cubes same as the basic CaCO_3 nanoparticles. This confirms that the shape of nanoparticles used as core is governed by the shape of core shell nanoparticles. CaCO_3 nanoparticles were directly coated with a layer of silica by hydrolysis and condensation of Na_2SiO_3 in aqueous solution.

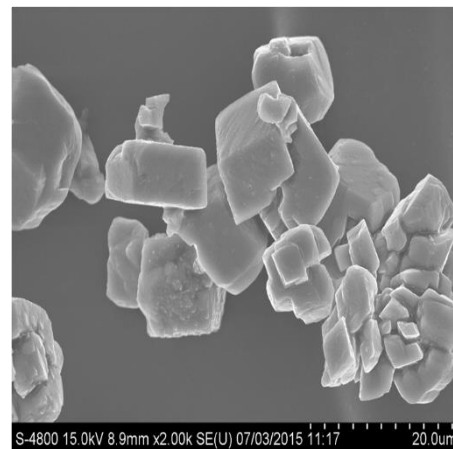


Figure 1. SEM image of $\text{CaCO}_3/\text{SiO}_2$ core shell nanoparticles revealing morphology.

3.2. XRD

The shape and size of $\text{CaCO}_3/\text{SiO}_2$ core shell nanoparticles were evaluated by XRD. The analysis of crystal structure using XRD illustrates the strong and sharp peaks showed that the nanoparticles was well crystalline. The average crystallite size (D) of the $\text{CaCO}_3/\text{SiO}_2$ core shell nanoparticles was calculated using Scherer's formula.

$$D = \frac{0.9\lambda}{\beta \cos\theta} \quad (7)$$

Where, shape factor is D , x-ray wavelength is λ , FWHM of diffraction peak is β , Bragg angle is θ .

The average crystallite size (D) of the calcium carbonate was calculated using Scherer's formula and was found to be 32 nm. It was concluded from Figure 2 that all of the peaks obtained in the XRD pattern of $\text{CaCO}_3/\text{SiO}_2$ core shell nanoparticles matched perfectly with the standard CaCO_3 pattern as is evident from. XRD image as given in Figure 2 of $\text{CaCO}_3/\text{SiO}_2$ core shell nanoparticles show that coating on CaCO_3 does not change the crystal structure of CaCO_3 core (Klugg & Alexander, 1974).

3.3. FE-SEM

3% loading of $\text{CaCO}_3/\text{SiO}_2$ core shell nanoparticles were found to be aggregated together and the aggregation were detached from each other as shown in Figure 3a.

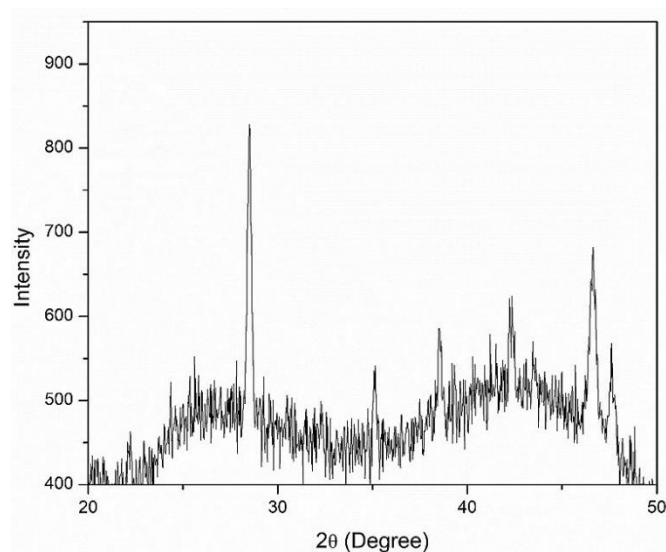


Figure 2. XRD of $\text{CaCO}_3\text{-SiO}_2$ core shell nanoparticles utilized for size evaluation.

With increasing $\text{CaCO}_3/\text{SiO}_2$ core shell nanoparticles loading, the amount of the aggregation increased as can be seen for 5% loading in Figure 3b. These aggregations comprised of several nanoparticles due to which their size reached micrometre level. Obviously, it was difficult to disperse nanoparticles homogeneously in the PC matrix through compounding PC pellets with $\text{CaCO}_3/\text{SiO}_2$ core shell nanoparticles during the melt extrusion processing (Sen et al., 2018).

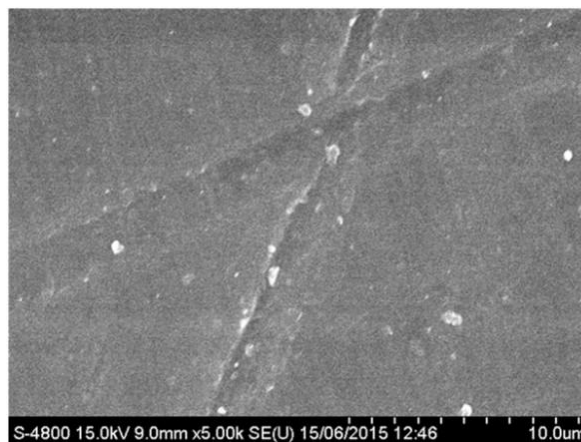


Figure 3a. FE-SEM images of polycarbonate composites representing 3% loading of nanoparticles.

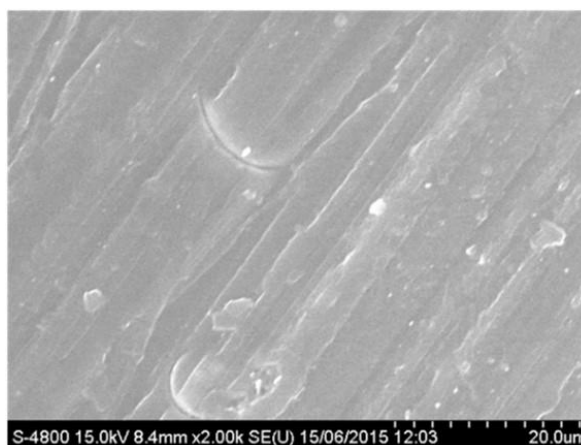


Figure 3b. FE-SEM images of polycarbonate composites representing 5% loading of nanoparticles.

3.4. Thermal properties

Thermal degradation of pure PC and polycarbonate/ $\text{CaCO}_3\text{-silica}$ core shell composites (polycarbonate composites), confirmed a two-stage process as is evident from Figure 4a. The reinforcement of core shell nanoparticles did not lead to any significant enhancement in thermal stability of the polycarbonate composites. From Table 1, it was observed that the onset of degradation for the case of polycarbonate composites was at a lower temperature as compared to the pure PC. This behaviour indicated a decrement as the concentration of nanoparticles increased. But the early degradation has also resulted in higher charred residue for the polycarbonate composites, indicating probable improvement in flame resistivity (Sonawane et al., 2009a; 2009b).

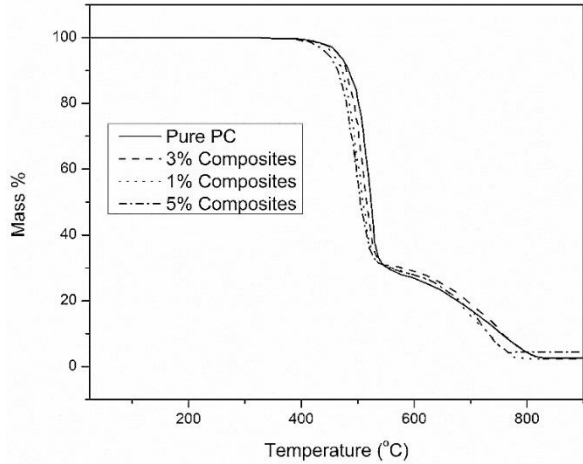


Figure 4a. TGA curves for evaluation of thermal stability of polycarbonate composites and pure PC.

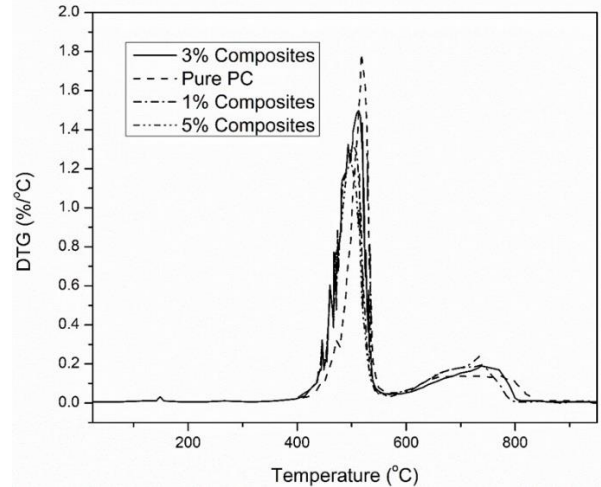


Figure 4b. DTG curves confirming number of stages of degradation.

Table 1. TGA data as obtained for PC and polycarbonate composites.

Sample		$T_{on\ set}(^{\circ}C)$	$T_{0.5}^{\circ}C$	Charred Residue
PC		461	519	0.8%
PC+	1%CaCO ₃ -SiO ₂ CS	459	505	0.8%
PC+	3%CaCO ₃ -SiO ₂ CS	447	498	2.8%
PC+	5%CaCO ₃ -SiO ₂ CS	436	491	2.7%

The DTG curve as is shown in Figure 4b, confirmed two stage degradation process of pure PC and polycarbonate composites. Also, the DSC endotherms depicted by Figure 4c, specified that the glass transition temperature values (T_g) of polycarbonate composites are nearly similar as that of pure PC. The T_g did not improve which confirmed the thermal stability decrement, as is observed by TGA. It means that presence of nanomaterials could not restrict the mobility of PC chain segments, indicating a poor reinforcement. T_g values did not change much, which can be confirmed with Tan Del curves. Table 2 displays a comparison of T_g values (Sonawane et al., 2010).

Table 2. DSC results for PC and polycarbonate composites.

Sample	PC	PC/CaCO ₃ -SiO ₂		
$T_g(^{\circ}C)$	Pure	1%	3%	5%
	150	148.6	149	148

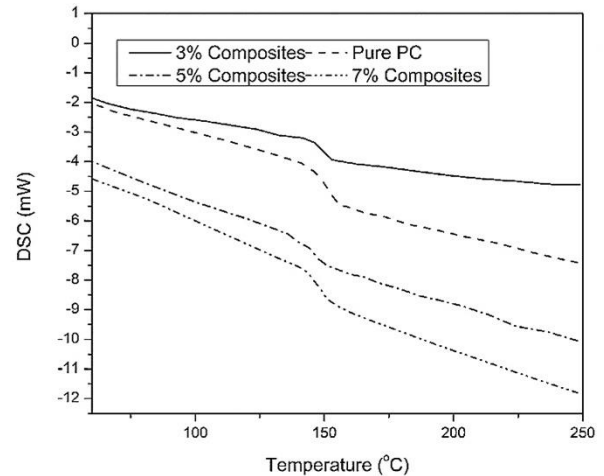


Figure 4c. DSC endotherms to evaluate the glass transition temperature (T_g).

3.5. Thermo-mechanical properties

The calcium carbonate-silica core shell nanoparticles were modified using stearic acid to achieve a good compatibility with the polycarbonate matrix. Polycarbonate composites were prepared at 280°C in an extruder using counter current screw arrangement. Figure 5a and 5b represent the results obtained from DMA. Figure 5a shows dependence of storage modulus on filler composition with temperature for polycarbonate composites. It is observed that the storage modulus of composites increases with the percentage composition thus leading to increase in stiffness of the material but only in the room temperature region. It is also clear that storage modulus for 5% polycarbonate composites confirmed maximum enhancement. The transition value of 5% polycarbonate composites is slightly lower than that of 1% and

3%. This is supported by Figure 5b where the peak points represent T_g and it is higher for 1% and 3% polycarbonate composites. When the reinforcement of nanoparticles in the polymer matrix is good, the damping effect represented by the peak in Figure 5b should decrease with percentage composition leading to better T_g . The dynamic mechanical properties depend on several factors i.e., filler's size, morphology and the extent of interaction between the filler and the polymer matrix. Here in spite of the presence of surface modifier, the T_g values did not improve, and the reinforcement achieved is low. The reason could be the catalysis of degradation due to a degradation of surface modifier at the processing temperature which is high. It is thus confirmed that the presence of higher percentage of nanoparticles did not lead to a restriction of polymer chain mobility. If this behaviour can be predicted using ANN a lot of time and money could be saved (Shimpi, Borane et al., 2018; Ghanshyam et al., 2016b).

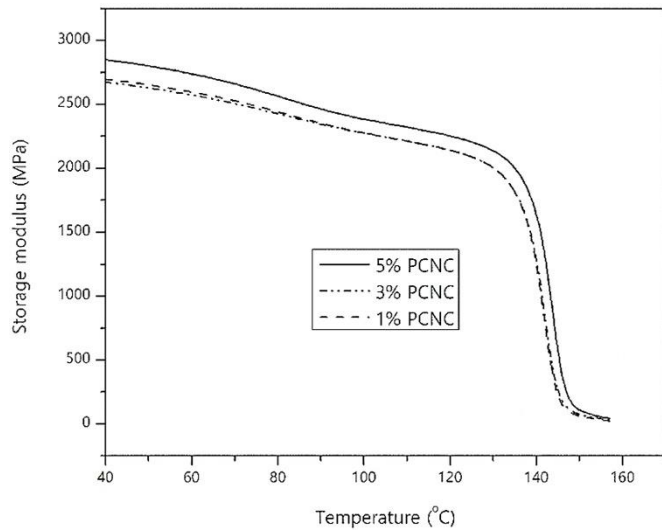


Figure 5a. DMA curves to evaluate storage modulus of polycarbonate composites.

3.6. Designing ANN model

A neural network, in its broadest sense, is made up of a number of neurons that, when combined, can perform any constructed function. To improve results, a sufficient training set should be identified. Approximately 70% of the data set is used for operating system training, with the remaining 30% divided between testing and validation. The input layer, the hidden layer, and the output layer comprise the three layers of an ANN. Every neuron has three components: a normalised input, a transfer function, and an output. The network's neuron is stimulated by the weighted number of inputs, and one outcome is sent to the output units. The network will continue to operate until a convincing measurement accuracy is achieved. The data obtained from dynamic mechanical analyzer are in large volume, which is preferred for ANN

applications. The data was obtained for a system of PC/calcium carbonate-silica core shell composites with various compositions of nanoparticles like 1%, 3% and 5%.

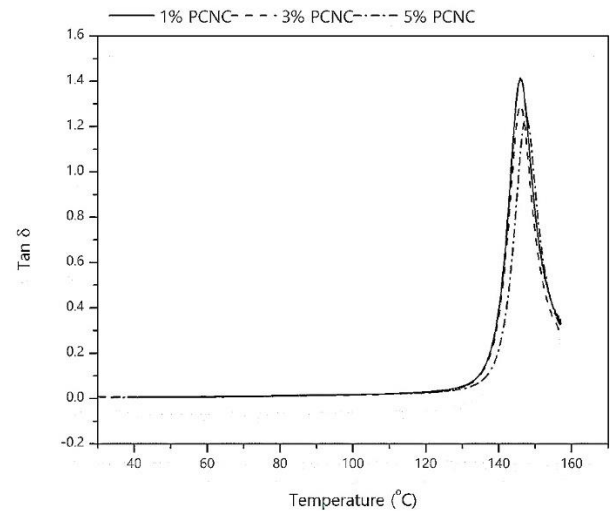


Figure 5b. Damping effect of the nanoparticles on the polycarbonate composites.

The datasets were used to train various developed ANN model. The data were separated as the training data set and validation data and the values are listed in supplementary Table S1. The data were normalized to obtain dimensionless parameters within a certain range using eq. 8.

$$y = \frac{x - x_{min}}{x_{min_{max}}} \quad (8)$$

Where, the normalization value is y , the original value is x . The maximum original value is x_{max} . The x_{min} is the minimum original value

Thus, the collected data using the normalization technique were processed. The same data was used to design neural network models to predict thermo-mechanical properties. The process of designing included a sequence of trials with several neural configurations along with layer and the function configuration. These models were compared, and the most successful model selected.

The different transfer functions available are *purelinear*, *tansigmoid* and *log sigmoid*. The function used for the second layer input to output is *purelinear* as it can generate the output in any numerical values, whereas *tansigmoid* and *logsigmoid* can generate outputs of either 1 or 0. The algorithm used to train the network was Levenberg-Marquardt algorithm (*TrainLM*). For most of the systems, the highest accuracy in prediction was provided by *TrainLM*. The training of models up to 1000 epochs using training dataset was an integral part before selecting any model. Epochs can be defined as number of times an ANN model is permitted to regulate the weight and bias

to accomplish better simulation. A better performance using the single-layer models was observed in training as compared to the multiple layer models. In single layer models, large models as compared to smaller models were confirmed to be comparatively better, e.g. 2-[4]-1. It was found that as the hidden layer increases in size like more than 4 neurons, no further enhancement in performance is expected. The single layer model with number of neurons as 4, was selected for the hidden layer as shown in Figure 6a.

The final model was selected when the system gradually converged and further improvement in performance was not observed anymore. It was observed that as the training cycles increased the error percentile dropped sharply. The parameter settings for ANN model are mentioned in Table 3.

Table 3. Parameter settings for ANN based Prediction model.

Neural network parameters	Selected values
Input layer neurons	2
Number of hidden layers	1
Number of neurons in the hidden layers	4
Number of neurons in the output layer	1
Activation function of hidden layers	Tansig
Activation function of output layers	Purlin
Training algorithm	Levenberg-Marquardt
Number of epochs	1000

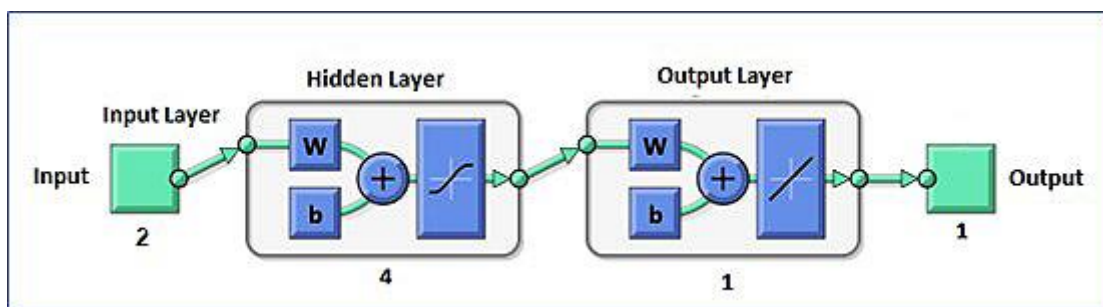


Figure 6a. ANN network structure selected for the system study.

3.6.1. Comparison of experimental and ANN results

By comparing the experimental values with its corresponding predicted values as obtained by using ANN model, the final model was tested and validated. Figure 6b represents all prediction set with training, validation and test and the regression (R) was found to be close to 1. In all the cases it was observed that the values of R were close to 1, indicating the fact that the suggested ANN model was precise in predicting $\tan \delta$ values. This also proves that the ANN model is capable of predicting the thermo-mechanical properties of polycarbonate composites (Sarve et al., 2015). Figure 6c represents the performance curve and it shows that performance converges to the range of 10^{-6} with 272 epochs. The experimental results were found to be in good relationship with the predicted values for all the parameters tested here with a high regression coefficient of 0.9999. Figure 7 shows assessment of experimental and ANN outputs when compared. It was observed that the coefficient of correlation is also close to 1 depicting the fact that the model used is the most suitable for the said system.

3.6.2. Prediction of thermo-mechanical properties for sample data

Using the established ANN model, it was easier to predict the $\tan \delta$ values i.e., thermo-mechanical properties for a given sample inputs with different concentrations of PCNC. Table 4 shows the data set used for testing the model along with experimental and predicted values of $\tan \delta$. The experimental and predicted properties follow the same trend with a correlation coefficient of 0.992 as shown in Figure 8. This value of correlation coefficient indicates the capability of the model to predict the results.

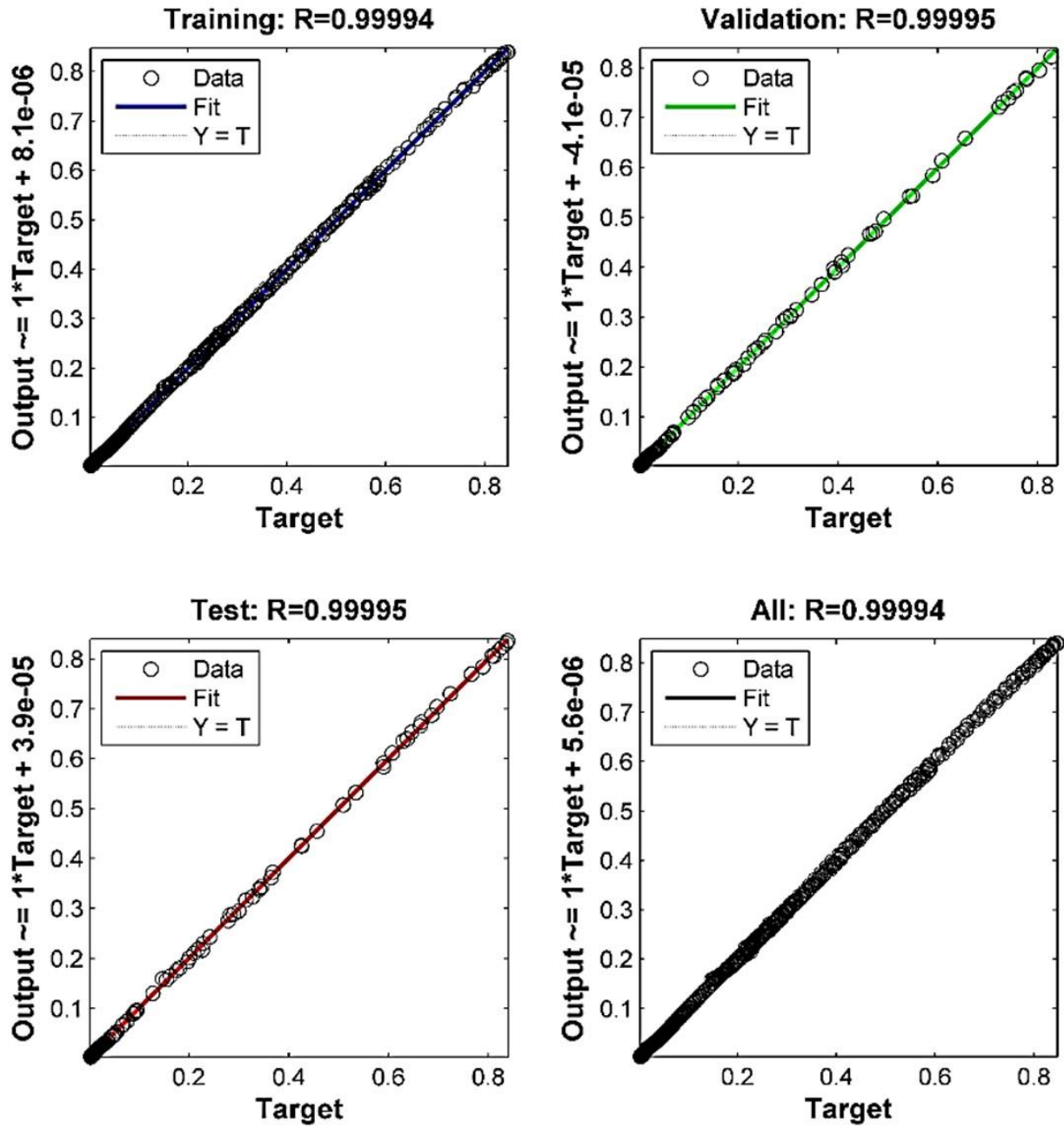


Figure 6b. Correlation between target and network outputs during training, its validation and testing together.

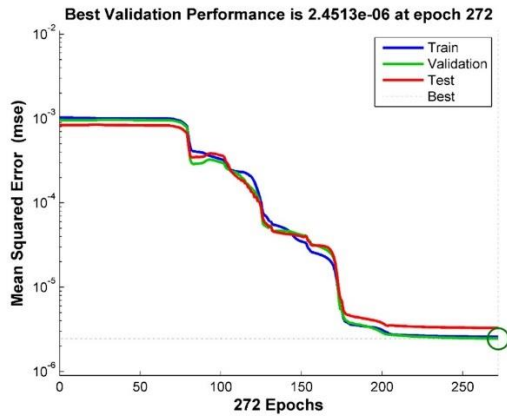


Figure 6c. Performance curve showing number of epochs and convergence of mean squared error.

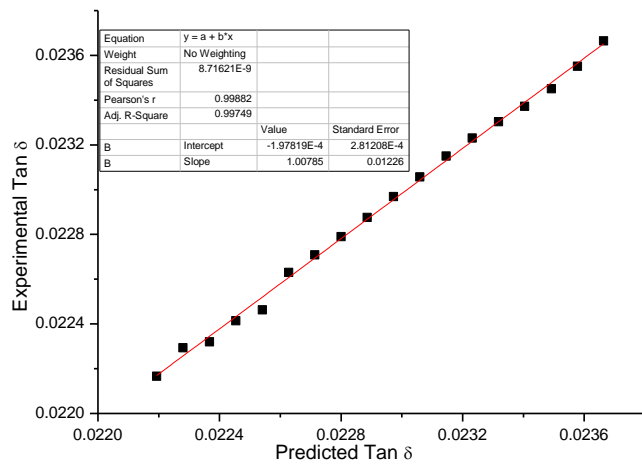


Figure 7. Comparison between experimental output and ANN predicted output.

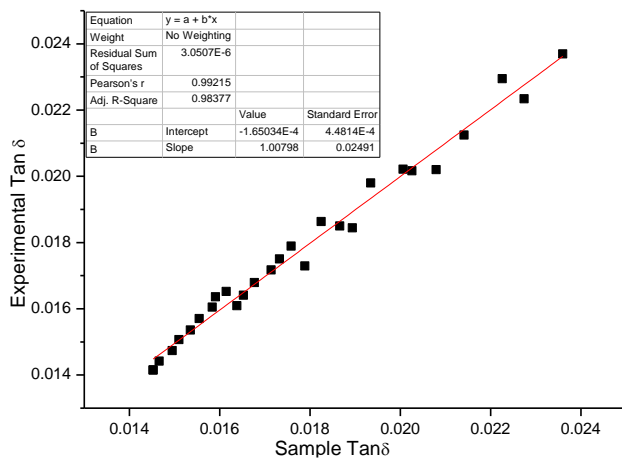


Figure 8. Comparison of experimental output with the ANN output for unseen data.

3.6.3. Prediction of $\tan \delta$ for an unknown concentration 2% PCNC

The prediction capability of the ANN model is checked using an unknown concentration of 2% PCNC. The results obtained using the designed ANN model is listed in table 4. The values when compared to the experimental outputs of 3 % PCNC are close to the expected range which proves that the model is the most suitable for prediction of thermo-mechanical properties of polycarbonate composites.

3.6.4. Sensitivity analysis

The weights used for sensitivity analysis is obtained from the ANN model. In the biological sciences, the strengths between the axons and dendrites are equivalent to these weights. Subsequently the percentage of the input signal which should be transmitted into the body of neurons, will be decide by each weight (Slokar et al., 1999). The comparative significance of the three input variables is listed in Table 5. The relative importance of temperature at which load is being applied is more than the other variable but they help in learning the system faster for better performance. In absence of these the system takes longer time to converge, and generalization obtained is not good (Shimpi et al., 2011; Charde, Sonawane, Sonawane, & Navin, 2018).

3.6.5. Prediction of Glass transition temperature using optimization by genetic algorithm

Figure 9 demonstrates the effects of temperature and concentration on the $\tan \delta$ values in 3D. The ANN model was used to optimize the conditions using genetic algorithm. It is observed that $\tan \delta$ values are almost constant up to a temperature of 130°C very close to its transition value. A step increase in the values is observed up to a maximum value of $\tan \delta=1.2$. This peak value corresponds to the glass transition temperature of the polycarbonate composite for a concentration of 5% PCNC and it is 147°C.

Table 4. Model tested for 1 and 2% composition of PCNC at 149°C peak temperature.

Concentration (%)	Temperature	Experimental Tan δ	Predicted Tan δ	% Error
1	93.13809	0.014528	0.014148	2.61564
1	94.03843	0.014662	0.014417	1.67099
1	95.08978	0.014947	0.014739	1.39158
1	96.14039	0.015097	0.015068	0.19209
1	97.04145	0.015352	0.015357	-0.03257
1	98.09259	0.015548	0.015701	-0.98405
1	99.1447	0.015834	0.016052	-1.37678
1	100.0445	0.015907	0.016358	-2.83523
1	101.0944	0.016144	0.01652	-2.32904
1	102.1443	0.01638	0.016089	1.77656
1	103.0436	0.016526	0.016409	0.70798
1	104.0937	0.016768	0.016788	-0.11927
1	105.1428	0.017139	0.017171	-0.18671
1	106.0427	0.017325	0.017503	-1.02742
1	107.0918	0.01758	0.017894	-1.78612
1	108.1418	0.017889	0.017289	3.35402
1	109.0426	0.01825	0.018631	-2.08767
1	110.0928	0.018659	0.01850034	0.85031
1	111.1484	0.018937	0.018443	2.60865
1	112.0485	0.019346	0.019797	-2.33123
1	113.0988	0.02006	0.020215	-0.77268
1	114.1486	0.020256	0.0201643	0.45271
1	115.0477	0.020795	0.0202018	2.85261
1	116.0984	0.021414	0.0212472	0.77893
1	117.1472	0.022258	0.022948	-3.10001
1	118.0479	0.022743	0.0223379	1.78121
1	119.0959	0.023599	0.0236919	-0.39366
1	93.13809	0.014528	0.014148	2.61564
2	108.0515	0.022193	0.022166	0.1230
2	108.2017	0.02228	0.021932	1.5600
2	108.3514	0.022367	0.021992	1.6780
2	108.5018	0.022454	0.022414	0.1789
2	108.6518	0.022541	0.022263	1.2340
2	108.802	0.022628	0.021999	2.7800
2	108.9511	0.022714	0.022058	2.8900
2	109.0992	0.0228	0.022369	1.8900

2	109.2493	0.022886	0.022527	1.5678
2	109.3987	0.022973	0.022929	0.1907
2	109.5484	0.023059	0.022708	1.5210
2	109.6988	0.023146	0.022896	1.0780
2	109.8479	0.023232	0.023193	0.1678
2	109.9978	0.023318	0.02303	1.2350
2	110.148	0.023404	0.022725	2.9011
2	110.2999	0.023492	0.022809	2.9080
2	110.4499	0.023578	0.023169	1.7340
2	110.6006	0.023664	0.023341	1.3670

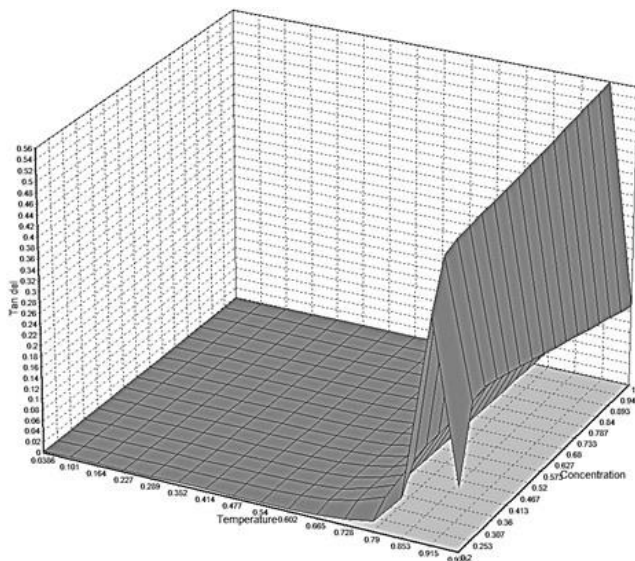


Figure 9. Three-dimensional plot showing the effects of temperature and concentration of nanoparticles

Table 5. Sensitivity analysis result as obtained from the ANN model.

Input Variables	Percentage of importance
Temperature (°C)	64.42
Concentration (%)	35.25

4. Conclusions

The current effort was an attempt to investigate the possibility of using an artificial neural network to precisely predict the thermomechanical properties of polycarbonate composites. The experimental results are found to be consistent with the

predictions of the ANN. This model is best suited for a system composed of polycarbonate composites, as the addition of filler results in a decrease in Tg values. Correlation coefficients that are high and mean squared error values that are small ensure that the training process is accurate. The uniform correlation coefficient values and close mean squared error values observed for the training, validation, and testing data sets indicate that the ANN model has a high degree of generalization competence. Tan values for unknown concentrations are also within the acceptable range. Optimization contributes to the determination of the glass transition temperature of polycarbonate composites. Thus, using an ANN model, it is possible to predict the thermomechanical properties of polycarbonate composites as a function of concentration and temperature. This prior knowledge is beneficial when determining the ultimate application for the new composite product. After the network is finalized, the time required is only a few seconds to a few minutes, making it a faster option than characterizations and testing, saving both time and money.

Conflict of interest

We on behalf of all the authors state that there is no conflict of interest as far as this manuscript is concern.

Acknowledgments

We acknowledge the support provided by our Hon'ble Director VNIT for infrastructural and equipment facility etc for this research work carried out.

Financing

There was no funding available for this research work carried in our laboratory.

References

- Aktay L, Johnson A F, Holzapfel M. (2005). Prediction of impact damage on sandwich composite panels. *Computational Material Science*, 32, 252–260.
<https://doi.org/10.1016/j.commatsci.2004.09.044>
- Carrion, F. J., Sanes, J., & Bermúdez, M. D. (2007). Influence of ZnO nanoparticle filler on the properties and wear resistance of polycarbonate. *Wear*, 262(11-12), 1504-1510.
<https://doi.org/10.1016/j.wear.2007.01.016>
- Carrión, F. J., Arribas, A., Bermúdez, M. D., & Guillamon, A. (2008). Physical and tribological properties of a new polycarbonate-organoclay nanocomposite. *European Polymer Journal*, 44(4), 968-977.
<https://doi.org/10.1016/j.eurpolymj.2008.01.038>
- Chau, J. L. H., Hsu, S. L. C., Chen, Y. M., Yang, C. C., & Hsu, P. C. (2010). A simple route towards polycarbonate–silica nanocomposite. *Advanced Powder Technology*, 21(3), 341-343.
<https://doi.org/10.1016/j.appt.2010.02.005>
- Charde, S. J., & Sonawane, S. S. (2016). Thermo mechanical properties of polycarbonate-OMMT clay nanocomposites using artificial neural network. In *2016 IEEE Nanotechnology Materials and Devices Conference (NMDC)* (pp. 1-2). IEEE.
<https://doi.org/10.1109/NMDC.2016.7777179>
- Charde, S. J., Sonawane, S. S., Rathod, A. P., Sonawane, S. H., Shimpi, N. G., & Parate, V. R. (2017). Copper-doped zinc oxide nanoparticles: Influence on thermal, thermo mechanical, and tribological properties of polycarbonate. *Polymer Composites*, 39(S3), 1398-1406.
<https://doi.org/10.1002/pc.24315>
- Charde, S. J., Sonawane, S. S., Sonawane, S. H., Shimpi N. G. (2018). Degradation Kinetics of Polycarbonate Composites: Kinetic Parameters and Artificial Neural Network. *Chemical and Biochemical Engineering Quarterly*, 32 (2), 151–165.
<https://doi.org/10.15255/CABEQ.2017.1173>
- Charde, S. J., Sonawane, S. S., Sonawane, S. H., & Navin, S. (2018). Influence of functionalized calcium carbonate nanofillers on the properties of melt-extruded polycarbonate composites. *Chemical Engineering Communications*, 205(4), 492-505.
<https://doi.org/10.1080/00986445.2017.1404459>
- Garson G. D. (1991). Interpreting neural-network connection weights. *AI Expert*, 6(4), 46–51.
- Ghanshyam, B., Sonawane Shriram, S., Wasewar Kailas, L., Rathod Ajit, P., Parate Vishal, R., Sonawane Shirish, H., & Shimpi Navin, G. (2016). Improvement in thermal stability, thermomechanical and oxygen permeability of PA6 by ODA modified Ca₃(PO₄)₂ nanofiller. *Research Journal of Chemistry and Environment*, 21(6), 38-44.
- Ghanshyam, B., Shriram, S. S., & Kailas, W. L. (2016a). Study on thermal and mechanical properties and crystallization behaviour of PA6, PVC and OMMT nanocomposites. *Research Journal of Chemistry and Environment*, 20(10).
- Ghanshyam, B., Shriram, S. S., & Kailas, W. L. (2016b). Effect of Octadecyl Amine modified MMT on Thermal Stability, Viscoelastic Properties and Crystallization Behaviour of Polyamide 6 Nanocomposites. *Research Journal of Chemistry and Environment*, 20 (11), 1-4.
- Ghanshyam, B., Sonawane Shriram, S., Wasewar Kailas, L., Rathod Ajit, P., Sonawane Shirish, H., & Shimpi Navin, G. (2017). Synthesis of CaSO₄ nanoparticles and its effect on PA6/CaSO₄ nanocomposite for investigation of thermal and viscoelastic properties. *Research Journal of Chemistry and Environment*, 21(11), 39-44.
- Jin, S. H., Choi, D. & Lee, D. S. (2008). Electrical and rheological properties of polycarbonate/multiwalled carbon nanotube nanocomposites. *Colloids and Surfaces A: Physicochemical and Engineering Aspects*, 313, 242-245.
<https://doi.org/10.1016/j.colsurfa.2007.04.104>
- Khan, K. M., & Khan, A. (2002). Catalytic reduction of NO with H₂ on a square surface: a Monte Carlo simulation study. *Journal of Physics: Condensed Matter*, 14(34), 7919.
- Khan, A., Shamsi, M. H., & Choi, T. S. (2009). Correlating dynamical mechanical properties with temperature and clay composition of polymer-clay nanocomposites. *Computational Materials Science*, 45(2), 257-265.
<https://doi.org/10.1016/j.commatsci.2008.09.027>
- Khan, M., Mishra, S., Ratna, D., Sonawane, S., & Shimpi, N. G. (2019) Investigation of thermal and mechanical properties of styrene–butadiene rubber nanocomposites filled with SiO₂–polystyrene core–shell nanoparticles. *Journal of Composite Materials*, 54 (14), 1-11.
<https://doi.org/10.1177/0021998319886618>

- Khanam, P. N., AlMaadeed, M. A., AlMaadeed, S., Kunhoth, S., Ouederni, M., Sun, D., ... & Mayoral, B. (2016). Optimization and prediction of mechanical and thermal properties of graphene/LLDPE nanocomposites by using artificial neural networks. *International Journal of Polymer Science*, 2016. <https://doi.org/10.1155/2016/5340252>
- Klug, H. P., & Alexander, L. E. (1974). *X-ray diffraction procedures: for polycrystalline and amorphous materials*. 2nd Edition. In *X-ray diffraction procedures*. John Wiley and Sons.
- Landge, V. K., Sonawane, S. H., Sivakumar, M., Sonawane, S. S., Babu, G. U. B., & Boczkaj, G. (2021). S-scheme heterojunction Bi₂O₃-ZnO/Bentonite clay composite with enhanced photocatalytic performance. *Sustainable Energy Technologies and Assessments*, 45, 101194. <https://doi.org/10.1016/j.seta.2021.101194>
- Lingaraju, D., Ramji, K., & Rao, N. M. (2011). Characterization and prediction of some engineering properties of polymer-Clay/Silica hybrid nanocomposites through ANN and regression models. *Procedia Engineering*, 10, 9-18. <https://doi.org/10.1016/j.proeng.2011.04.004>
- Luyt, A. S., Messori, M., Fabbri, P., Mofokeng, J. P., Taurino, R., Zanasi, T., & Pilati, F. (2011). Polycarbonate reinforced with silica nanoparticles. *Polymer bulletin*, 66(7), 991-1004. <https://doi.org/10.1007/s00289-010-0408-5>
- Majid, A., & Lee, Y. S. (2009). Predicting lattice constant of cubic perovskites using support vector regression. In *Proceedings of the 2nd International Conference on Interaction Sciences: Information Technology, Culture and Human* (pp. 175-183). <https://doi.org/10.1145/1655925.1655957>
- Malika, M., & Sonawane, S. S. (2021a). Statistical modelling for the Ultrasonic photodegradation of Rhodamine B dye using aqueous based Bi-metal doped TiO₂ supported montmorillonite hybrid nanofluid via RSM. *Sustainable Energy Technologies and Assessments*, 44, 100980. <https://doi.org/10.1016/j.seta.2020.100980>
- Malika, M., & Sonawane, S. S. (2021b). Application of RSM and ANN for the prediction and optimization of thermal conductivity ratio of water based Fe₂O₃ coated SiC hybrid nanofluid. *International Communications in Heat and Mass Transfer*, 126, 105354. <https://doi.org/10.1016/j.icheatmasstransfer.2021.105354>
- Mishra, S., Sonawane, S. S., & Shimpi, N. G. (2009a). Influence of organo-montmorillonite on mechanical and rheological properties of polyamide nanocomposites. *Applied Clay Science*, 46(2), 222-225. <https://doi.org/10.1016/j.clay.2009.07.024>
- Mishra, S., Sonawane, S. S., & Shimpi, N. G. (2009b). Effect of commercial & nano-Ca₃(PO₄)₂ on mechanical and thermal properties of polyamide composites. *Polymer-Plastics Technology and Engineering*, 48(3), 265-271. <https://doi.org/10.1080/03602550802674713>
- Motaung, T. E., Saladino, M. L., Luyt, A. S., & Chillura Martino, D. F. (2012). The effect of silica nanoparticles on the morphology, mechanical properties and thermal degradation kinetics of polycarbonate. *Composites Science and Technology*, 73, 34-39. <https://doi.org/10.1016/j.compscitech.2012.08.014>
- Nasir, T., Yousif, B. F., McWilliam, S., Salih, N. D., & Hui, L. T. (2010). An artificial neural network for prediction of the friction coefficient of multi-layer polymeric composites in three different orientations. *Proceedings of the Institution of Mechanical Engineers, Part C: Journal of Mechanical Engineering Science*, 224(2), 419-429. <https://doi.org/10.1243/09544062JMES1677>
- Sarve, A., Sonawane, S. S., & Varma, M. N. (2015). Ultrasound assisted biodiesel production from sesame (*Sesamum indicum* L.) oil using barium hydroxide as a heterogeneous catalyst: Comparative assessment of prediction abilities between response surface methodology (RSM) and artificial neural network (ANN). *Ultrasonics sonochemistry*, 26, 218-228. <https://doi.org/10.1016/j.ultsonch.2015.01.013>
- Sen, T., Mishra, S., Sonawane, S. S., & Shimpi, N. G. (2018). Polyaniline/zinc oxide nanocomposite as room-temperature sensing layer for methane. *Polymer Engineering & Science*, 58(8), 1438-1445. <https://doi.org/10.1002/pen.24740>
- Shimpi, N. G., Kakade, R. U., Sonawane, S. S., Mali, A. D., & Mishra, S. (2011). Influence of nano-inorganic particles on properties of epoxy nanocomposites. *Polymer-Plastics Technology and Engineering*, 50(8), 758-761. <https://doi.org/10.1080/03602559.2010.551437>
- Shimpi, N. G., Khan, M., Shirole, S., & Sonawane, S. (2018). Process Optimization for the Synthesis of Silver (AgNPs), Iron Oxide (α-Fe₂O₃NPs) and Core-Shell (Ag-Fe₂O₃CNPs) Nanoparticles Using the Aqueous Extract of *Alstonia Scholaris*: A Greener Approach. *The Open Materials Science Journal*, 12(1), 29-39. <https://doi.org/10.2174/1874088X01812010029>
- Shimpi, N., Borane, M., Mishra, S., Kadam, M., & Sonawane, S. S. (2018). Biodegradation of isotactic polypropylene (iPP)/poly (lactic acid) (PLA) and iPP/PLA/nano calcium carbonates using phanerochaete chrysosporium. *Advances in Polymer Technology*, 37(2), 522-530. <https://doi.org/10.1002/adv.21691>

- Sonawane S.S., Rathod A.P., Wasewar K. L., & Varma M.N. (2011). *Nanocomposites for Food Packaging Applications, Research Journal of Chemistry and Environment, 15 (2), 721-723.*
- Sonawane, S. S., Mishra, S., & Shimpi, N. G. (2009a). Effect of nano-CaCO₃ on mechanical and thermal properties of polyamide nanocomposites. *Polymer-Plastics Technology and Engineering, 49(1), 38-44.*
<https://doi.org/10.1080/03602550903204220>
- Sonawane, S. S., Mishra, S., & Shimpi, N. G. (2009b). Polyamide nanocomposites: investigation of mechanical, thermal and morphological characteristics. *Polymer-Plastics Technology and Engineering, 48(10), 1055-1061.*
<https://doi.org/10.1080/03602550903092583>
- Sonawane, S. S., Mishra, S., Shimpi, N. G., Rathod, A. P., & Wasewar, K. L. (2010). Comparative study of the mechanical and thermal properties of polyamide-66 filled with commercial and nano-Mg (OH)₂ particles. *Polymer-Plastics Technology and Engineering, 49(5), 474-480.*
<https://doi.org/10.1080/03602550903413938>
- Sonawane, S., Thakur, P., & Paul, R. (2020a). Study on thermal property enhancement of MWCNT based polypropylene (PP) nanocomposites. *Materials Today: Proceedings, 27, 550-555.*
<https://doi.org/10.1016/j.matpr.2019.12.018>
- Sonawane, S. S., Thakur, P. P., & Paul, R. (2020b). Study on visco-elastic properties enhancement of MWCNT based polypropylene nanocomposites. *Materials Today: Proceedings, 29, 929-933.*
<https://doi.org/10.1016/j.matpr.2020.05.417>
- Slokar Y M, Zupan J, L. M. A. M. (1999). The use of artificial neural network (ANN) for modelling of the H₂O₂/UV decoloration process: part 1. *Dyes and Pigments, 42(2), 123-135.*
[https://doi.org/10.1016/S0143-7208\(99\)00022-4](https://doi.org/10.1016/S0143-7208(99)00022-4)
- Suin, S., Shrivastava, N. K., Maiti, S., & Khatua, B. B. (2013). Phosphonium modified organoclay as potential nanofiller for the development of exfoliated and optically transparent polycarbonate/clay nanocomposites: Preparation and characterizations. *European polymer journal, 49(1), 49-60.*
<https://doi.org/10.1016/j.eurpolymj.2012.10.004>
- Yegnanarayana, B. (2009). *Artificial neural networks.* PHI Learning Pvt. Ltd.
- Zhang, Z., Klein, P., & Friedrich, K. (2002a). Dynamic mechanical properties of PTFE based short carbon fibre reinforced composites: experiment and artificial neural network prediction. *Composites Science and Technology, 62(7-8), 1001-1009.*
[https://doi.org/10.1016/S0266-3538\(02\)00036-2](https://doi.org/10.1016/S0266-3538(02)00036-2)
- Zhang, Z., Friedrich, K., & Velten, K. (2002b). Prediction on tribological properties of short fibre composites using artificial neural networks. *Wear, 252(7-8), 668-675.*
[https://doi.org/10.1016/S0043-1648\(02\)00023-6](https://doi.org/10.1016/S0043-1648(02)00023-6)
- Zhang, S., & Li, X. (2004). Synthesis and characterization of CaCO₃@SiO₂ core-shell nanoparticles. *Powder technology, 141(1-2), 75-79.*
<https://doi.org/10.1016/j.powtec.2004.02.018>